American Mineralogist, Volume 65, pages 1075–1086, 1980

Anthophyllite asbestos: microstructures, intergrown sheet silicates, and mechanisms of fiber formation

DAVID R. VEBLEN

Department of Geology, Arizona State University
Tempe, Arizona 85281

Abstract

The complex microstructures of an anthophyllite asbestos specimen from Pelham, Massachusetts, have been elucidated by transmission electron microscopy and electron diffraction techniques. The specimen consists primarily of small amphibole crystallites that are greatly elongated in the *c* direction. Adjacent crystallites are crystallographically rotated with respect to each other, but are not related by a twinning operation. The anthophyllite possesses pervasive moderate chain-width disorder. Central screw dislocations are not present in the crystallites, indicating that they did not grow by a spiral growth mechanism around screw dislocations.

The grain-boundary structures between rotated crystallites have been characterized using high-resolution TEM methods. Low-angle grain boundaries may be largely structurally coherent, whereas high-angle grain boundaries are typically incoherent. Many of the grain boundaries are partially filled by talc, serpentine minerals, or chlorite. Unusual conformations of curved serpentine are present, and antigorite occurs in ordered 1- and 2-layer polytypes that are intimately intergrown with stacking-disordered antigorite. The curvature reversals in some areas of antigorite are non-periodic, with spacings much larger than those usually observed.

The microstructures strongly suggest that the primary mechanism of fiber formation in this asbestos is separation along the grain boundaries between individual crystallites. This process may be enhanced by the pervasive presence of sheet silicates along the grain boundaries. However, this is not the only mechanism of fiber formation that can occur in amphiboles, since in some other anthophyllite specimens crystals split preferentially along (100) stacking faults and (010) chain-width errors. Disaggregation along such planar defects may thus be an important secondary mechanism of fiber formation in commercial amphibole asbestos.

The correlation of chain-width errors with the asbestiform habit may result in part from the cellular structure of amphibole asbestos: hydrothermal fluids that produce these defects could diffuse much more rapidly along the incoherent grain boundaries than they could through the bulk structure of massive amphiboles. Rapid fluid conduction along these cellular grain boundaries can also account for the abundance of sheet silicates as grain-boundary fillings.

Introduction

Some of the most complex problems in mineralogy involve the relationships among physical properties, crystal structure, and defect structure. In many minerals, the ideal crystal structure clearly controls mechanical properties, such as cleavage, as well as other properties, such as color and electrical conductivity. In other cases, crystal defects exercise controlling influences on physical properties. For example, low concentrations of the defects referred to as color centers can severely alter light-absorption properties of alkali halides, and the mechanical deformation properties of most crystalline materials are dependent as much on the presence and motion of dislocations as they are on the ideal crystal structure.

One of the most important unanswered questions in rock-forming silicate crystallography involves the mechanical behavior of amphiboles. Most amphibole crystals ("massive or acicular amphiboles") are quite brittle and when broken exhibit excellent prismatic cleavage. On the other hand, some amphibole specimens ("amphibole asbestos") are not at all brittle

0003–004X/80/1112–1075$02.00

and are easily disaggregated into strong, flexible fibers with pronounced elongation in the *c* direction. Why is there this duplicity of mechanical properties among the amphiboles, when both massive and asbestiform types apparently have the same basic crystal structure and chemical characteristics? Perhaps the differences in properties result from microstructural differences arising either during primary growth or during subsequent alteration of the amphibole. Accordingly, I aim to identify the kinds of defects that lead to asbestiform habit in anthophyllite, which is just one of numerous amphiboles that can occur either as massive crystals or as asbestos.

Defect control of amphibole habit has been discussed previously by Veblen *et al.* (1977), who suggested that asbestiform amphiboles selectively break along the (100) twin planes or stacking faults, or along the chain-width errors that are abundant in some occurrences (Veblen and Burnham, 1978a,b; Veblen and Buseck, 1979a, 1980). Alario Franco *et al.* (1977) showed, on the other hand, that the fibrils in commercial-grade crocidolite (riebeckite asbestos) consist of individual crystallites that are elongated in the *c* direction and are rotated with respect to each other about the [001] direction. X-ray study of fibers of a South African amosite (cummingtonite–grunerite asbestos) similarly showed extreme misorientation about the *c* axis (Zoltai, 1979). In these cases, the primary mechanism of fiber formation is presumably separation of the individual crystallites along the grain boundaries that separate them. However, published reports suggest that commercial amphibole asbestos specimens also contain a much higher concentration of chain-width errors and twinning or stacking faults than their massive counterparts (Chisholm, 1973, 1975; Hutchison *et al.*, 1975; Veblen *et al.*, 1977; Alario Franco *et al.*, 1977; Veblen and Buseck, in preparation), and possibly these defects contribute to the fibrous habit or are intimately connected to the genesis of the rotated fibrils. On the other hand, Walker and Zoltai (1979) have compared amphibole asbestos fibers with synthetic whiskers and have suggested that a low density of surface defects may be important for asbestos properties.

There are thus several different hypotheses to explain the differences between massive and asbestiform habit in amphiboles. In this paper, new experimental evidence on anthophyllite is presented, and previously published reports are discussed in light of this problem. This evidence leads to the conclusion that there is no single mechanism for the formation of fibers in anthophyllite asbestos. Instead, several microstructural characteristics, operating either alone or in concert, can lead to the asbestiform habit.

The anthophyllite asbestos examined also contains finely intergrown talc and serpentine minerals, which were presumably produced during retrograde metamorphism of the amphibole. Although the intergrowths are in some ways similar to those reported previously in non-asbestiform specimens (Veblen and Buseck, 1979b; in preparation), this study reveals further variations in serpentine combination structures involving antigorite, chrysotile, and lizardite. The presence of pervasive minor alteration to sheet silicates presumably also affects the mechanical disaggregation properties of anthophyllite asbestos.

Specimens and experimental technique

Most of the work was performed with an anthophyllite asbestos specimen collected at the Pelham Asbestos Mine, near Pelham, Massachusetts, while on an amphibole excursion led by Professor Peter Robinson. This specimen appears to be typical of the anthophyllite from this locality, which occurs as large blocks up to about a meter long in the fiber direction; these blocks were left lying around the mine after cessation of quarrying operations. The asbestos blocks are coherent and appear splintery, but when crushed they form fine, flexible, silky asbestos fiber. A parting cutting the anthophyllite *c* axis limits the length of individual milled fibrils to about one centimeter.

Thin specimens for high-resolution transmission electron microscopy were prepared by argon-ion-milling pieces of a petrographic thin section cut normal to the fibers. Electron microscopy was performed with a JEOL JEM100B microscope, as described by Veblen and Buseck (1979a). Images were interpreted as described in Veblen *et al.* (1977) and Veblen and Buseck (1979a,b; 1980).

The above specimen will be compared with other anthophyllite specimens that have already been described: anthophyllite from the Cascades, Washington (Veblen and Buseck, 1979b), and anthophyllite from Chester, Vermont (Veblen and Burnham, 1978a,b; Veblen *et al.*, 1977; Veblen and Buseck, 1979a, 1980).

Microstructures in Pelham anthophyllite

Chain-width disorder

The Pelham anthophyllite contains significant numbers of chain-width errors, primarily with chain widths of three, four, five, and six. The wide-chain

material accounts for only a few percent of the total chain silicate, however, and no ordered domains of chesterite or jimthompsonite were observed. In low-resolution images the chain-width errors, which are parallel to (010), provide useful markers of crystallite orientation.

In most cases, the terminations of (010) lamellae of anomalous chain width, or "zippers," obey the coherent zipper termination rules of Veblen and Buseck (1979c, 1980). Rule violations that are accompanied by structural distortion are, however, a little more common in the Pelham anthophyllite asbestos than they are in the anthophyllite occurrence at Chester, Vermont. An example of such a violation is shown in Figure 1a, where a quadruple-chain zipper replaces an anthophyllite slab two chains wide. Thus, an odd number of chains (one) replaces an even number (two), in violation of the second termination rule. As in other amphiboles with chain-width disorder, zipper terminations are typically clumped together, along with associated displacive planar faults, as shown in Figure 1b. Such multiple terminations occur preferentially near grain boundaries.

Orientation relationships and crystallite size

Unlike anthophyllite specimens described previously, the Pelham anthophyllite asbestos consists of very small crystallites that have their *c* axes fairly well aligned in the fiber direction and that are rotated with respect to each other around the fiber direction. In this respect this specimen is microstructurally similar to the Australian crocidolite described by Alario Franco *et al.* (1977) in a HRTEM study and to the South African amosite examined by Zoltai (1979), the microstructure of which was inferred from an X-ray experiment. In the Pelham specimen, angular relationships among the *a* and *b* axes of adjoining crystallites appear to be random and clearly are not controlled by a twinning operation. The orientation relationships can be deduced from selected-area electron diffraction patterns from several crystallites, as shown in Figure 2. This pattern shows (*hk*0) diffractions from four anthophyllite crystals in different orientations, as well as light streaks arising from intergrown sheet silicate with stacking disorder. The patterns are not centered about the central beam, indicating that the *c* axes of the different anthophyllite crystallites are slightly misaligned. High-resolution imaging further substantiates these orientation relationships.

Individual crystallites are greatly elongated in the *c* direction. Their diameters in the specimens observed in the TEM range from a few hundred Å to a few micrometers, with most of the diameters falling

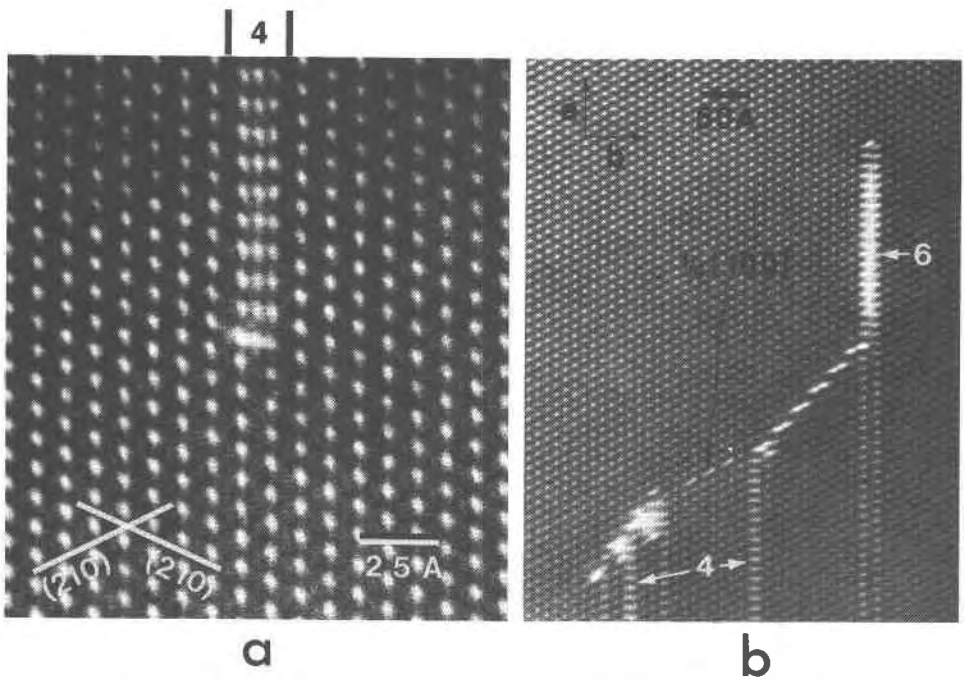

Fig. 1. (a) A slab of quadruple-chain silicate terminating in anthophyllite. This "zipper" terminates without producing an additional planar fault, and as a result produces structural distortion in the region of the termination. This distortion can be observed by sighting along the white spots at a low angle in the directions of the traces of the (210) planes. (b) A clump of terminating zippers, some of which are associated with additional planar faults having projected displacements of 1/4[100].

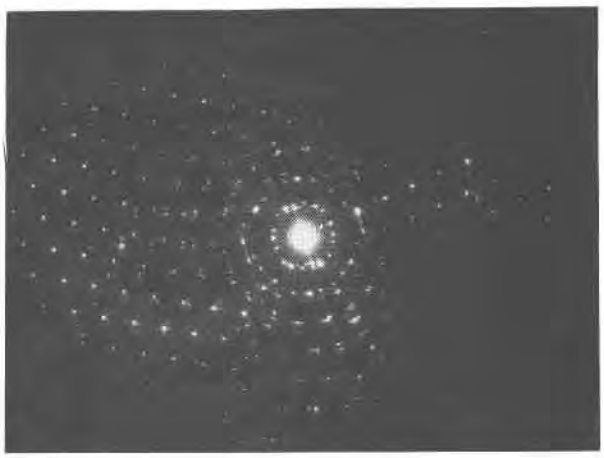

Fig. 2. An electron diffraction pattern from four anthophyllite crystallites in different orientations. The individual patterns are not centered about the central beam, but are displaced in various directions, showing that the c axes of the crystallites are not perfectly parallel to each other. The light streaks are from stacking-disordered talc intergrown in one of the grain boundaries.

between 0.1 and 1.0μm. An example of a crystallite $0.06 \times 0.14\mu$m in cross section is shown embedded in a larger crystallite in Figure 3. In petrographic thin section, regions with optically unresolvable crystallites are interspersed with areas having crystals from a few micrometers up to half a millimeter in diameter (Fig. 4); it is the finer-grained material that was examined in the electron microscope.

The microstructure of the Pelham anthophyllite, with its long, thin, rotationally-disordered crystallites, is a curious one and raises the question of a growth mechanism for the rotated fibrils. The most likely explanation involves a pervasive nucleation event along an opening fracture. Nuclei oriented with the fastest growth direction (c) nearly normal to the fracture would grow as the fracture opened, while crystallites in other orientations would not propagate. Such a mechanism is consistent with the slight c-axis misorientation among crystallites in the Pelham asbestos. Walker and Zoltai (1979) suggested that amphibole asbestos fibers, like some synthetic whiskers, are produced by spiral growth about a central screw dislocation. Though plausible, this mechanism would require each crystallite to possess a screw dislocation; contrast arising from such screw dislocations was not observed in the hundreds of fibers imaged with HRTEM in this study. An extensive search using conventional TEM techniques similarly failed to demonstrate the presence of any such dislocations having displacement components parallel to [001]. With rare exceptions, zipper terminations that could conceivably act as cores for spiral growth are likewise absent. It thus seems unlikely that the elongation of

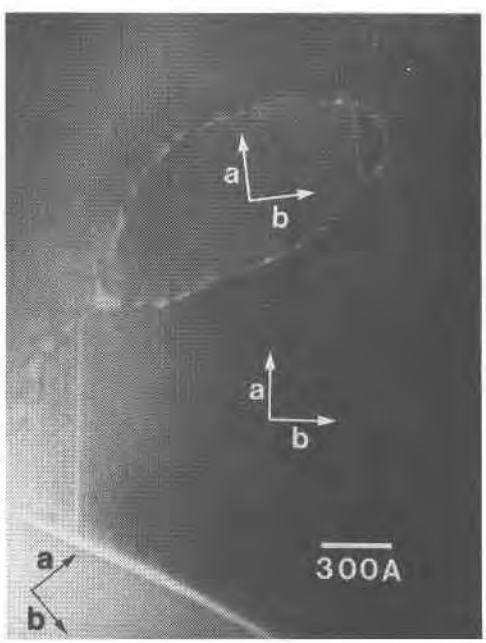

Fig. 3. Three different crystallites are indicated by the orientations of their a and b axes. The small crystallite in the upper part of the figure is completely surrounded by the large crystal that takes up most of the figure. The grain boundary between these two crystals is the closed oblong white line.

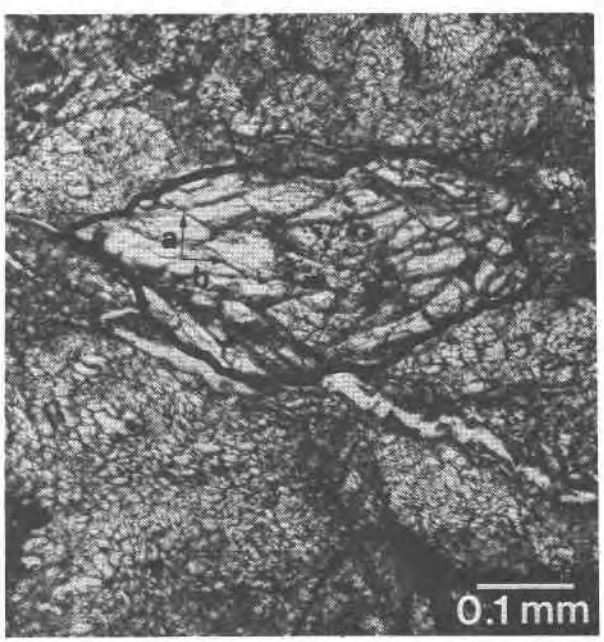

Fig. 4. Petrographic thin section of a relatively coarse-grained portion of the Pelham anthophyllite asbestos. One large single crystal (~0.5mm wide) is outlined in black. This large crystal is surrounded by numerous small crystallites having variable rotations about their c axes. Plane polarized light.

amphibole asbestos fibers can be attributed to spiral growth, at least in the present specimen.

Grain-boundary structures

Several different types of grain-boundary structures are observed between crystallites in the Pelham anthophyllite. The variations in structure are, in part, related to the orientation differences between adjoining grains. Where the orientation difference between two crystallites is very small, the interface is commonly a simple low-angle grain boundary that is mostly coherent, with partial dislocations absorbing the structural misfit (Fig. 5a; the relative rotation between the two crystals is about 0.5°). With larger differences in orientation between adjoining crystallites, structural coherency is lost, at least for most interface orientations (Fig. 5b; the relative rotation between the two crystals is about 9°).

Many grain boundaries between crystallites, however, are not simple amphibole–amphibole interfaces like those shown in Figures 5a,b. Instead, most of the high-angle grain boundaries, and also some of those with low angles, are at least partially filled with sheet silicates that include talc, serpentine minerals, and chlorite. An overview of the boundaries between three crystallites is shown in Figure 5c. At such boundaries containing sheet silicates, the interfaces between the sheet mineral and one of the crystallites usually exhibit strong structural control; these controlled interfaces are generally planar, while the interface of the sheet silicate with the other crystallite is irregular or ragged. The relationships between talc and anthophyllite at the controlled interfaces are typically the same as those commonly observed between talc and pyribole at Chester, Vermont (Veblen and Buseck, 1980): (1) $a_{tc} \parallel c_{an}$, $b_{tc} \parallel b_{an}$, and $c^*_{tc} \parallel a_{an}$; or (2) $(001)_{tc} \parallel (210)_{an}$. Boundaries having the first orientation relationship are typically parallel to (010), (210), or (100) of the anthophyllite. Where the sheet silicate occupying the boundary between anthophyllite crystallites is chlorite or serpentine, (001) of the sheet silicate is commonly parallel to (210) of the amphibole. This relationship is shown in Figure 5d, an interface between antigorite and anthophyllite; a large-scale undulation of the antigorite layers can also be seen in this figure.

Another grain-boundary relationship is shown in Figure 5e, where short talc layers are crystallographically related to one of the anthophyllite crystallites by relationship (1) above, but this controlled talc–amphibole interface is ragged rather than planar. In contrast, the boundary of the other anthophyllite crystallite is nearly planar and parallel to $(210)_{an}$. This situation is less common than those in which the crystallographically-controlled interface is planar. The fact that one of the anthophyllite boundaries is nearly always planar and has a rational crystallographic orientation of low index suggests that the interface energy is minimized by having one planar boundary and one ragged boundary, rather than two ragged boundaries with the sheet silicate. Another feature shown in Figure 5e is the local intercalation of 5Å layers in the talc; the structural configuration in such places is that of a chlorite mineral and has been observed in other occurrences where chain silicates have partially reacted to talc (Veblen and Buseck, 1980; in preparation).

Sheet silicates intergrown with Pelham anthophyllite

In addition to the features described in the last section on grain-boundary structure, there are many other fascinating microstructures in the sheet silicates in this asbestos specimen. In places, much of the anthophyllite has been replaced by talc and serpentine, so that there are sheet silicate grains in the tenth-micron size range, rather than simply as narrow grain-boundary fillings. Electron diffraction patterns indicate that this sheet silicate is oriented with its sheets more or less parallel to the pyribole silicate chains, as is typical in chain silicates that have partially reacted to sheet silicates. There is some variation in this orientation, however, just as there is variation in the orientations of the *c* axes of the anthophyllite, but the variations are not great enough to preclude simple interpretation of the HRTEM images.

The larger grains of talc are not very noteworthy. Like the talc that has been reported from intergrowths with pyroxenes, amphiboles, and wide-chain silicates from other localities, it exhibits stacking disorder in most areas, and the layers are commonly pulled apart locally (Veblen and Buseck, 1979b, 1980; in preparation).

The serpentine minerals, on the other hand, display remarkable diversity of structure. Like the fine-grained serpentine in certain uralites (Veblen and Buseck, 1979b), planar (lizardite) and curved (chrysotile) structures combine in some places to form complex patterns. More typical in this anthophyllite asbestos specimen, however, are curvature reversals in chrysotile, without the presence of lizardite structure. Figure 6 shows such microstructures in chrysotile that has grown, with talc, in two places along a low-angle (1.6°) grain boundary.

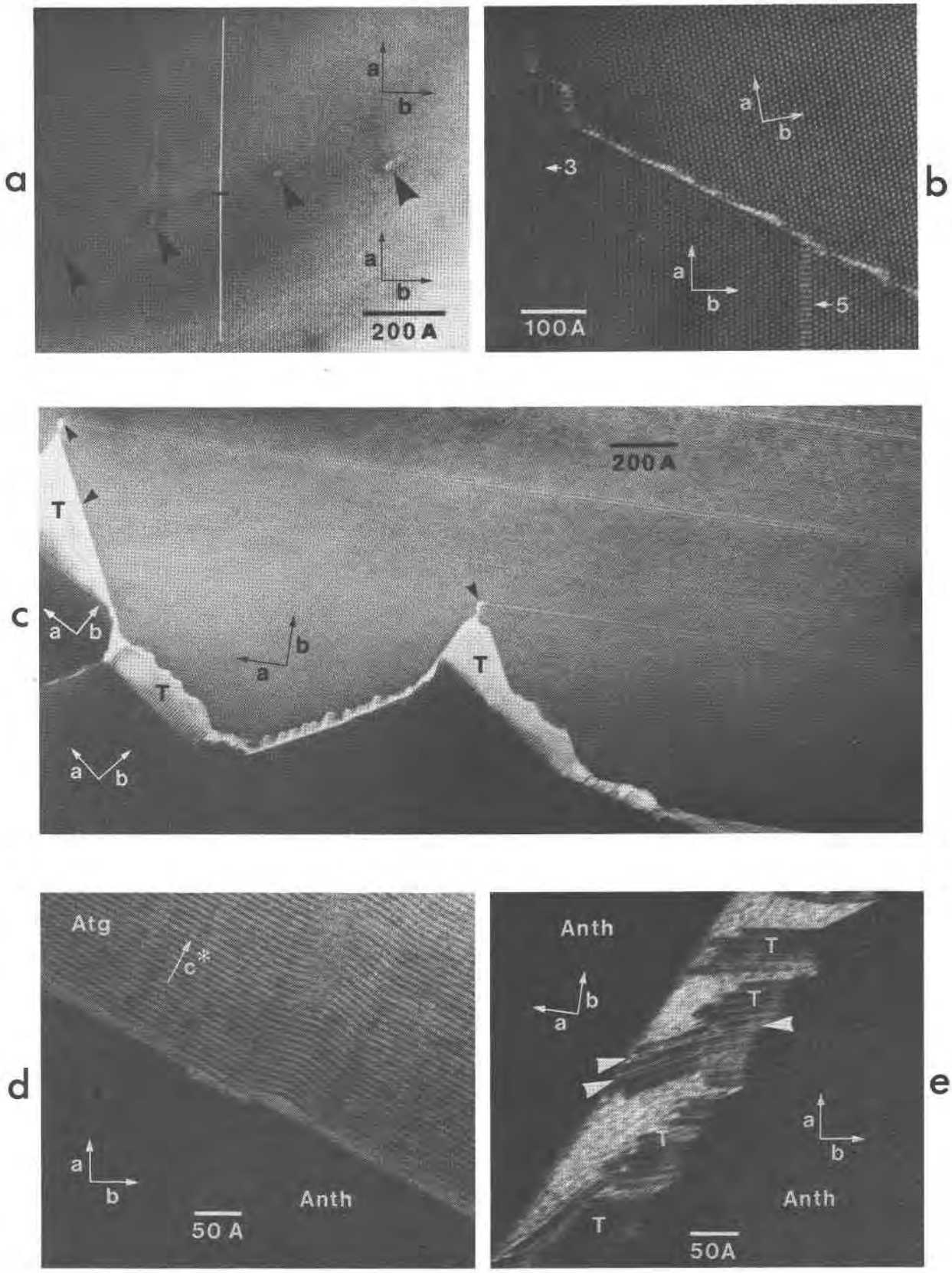
a
a
b
a
b
200 A
b
a
b
3
a
b
5
100 A
c
200 A
T
a
b
a
b
T
T
a
b
d
Atg
c*
a
b
Anth
50 A
e
Anth
T
a
b
T
T
a
b
Anth
50A

The most abundant serpentine mineral in this specimen is antigorite; the experimental imaging conditions for antigorite have been explored in some detail by Yada (1979). Yada found that image quality in antigorite was generally so poor that image processing techniques were required to produce interpretable photographs. This problem was not encountered in the present study, however, perhaps because of the low-damage methods used in specimen preparation. In some parts of the Pelham specimen, the antigorite occurs as undeformed crystals in which two different polytypes are intergrown. One of these is a one-layer polytype ($c \cong 7.3$Å), and the other is a two-layer polytype ($c \cong 14.6$Å). Multiple-layer polytypes of antigorite have been recognized only very recently (Yada, 1979; Arne Olsen, personal communication). Although Yada reported finding both a one-layer and a two-layer polytype in the same specimen, he did not observe the two polytypes intergrown in the same crystal. Figure 7, on the other hand, shows both stacking variations intergrown on an intimate basis. In addition, Figure 7 shows two heretofore unreported features in antigorite: both of the ordered polytypes contain isolated stacking faults, and the ordered antigorite is further intergrown with antigorite having disordered stacking. These features were not observed to change during exposure to the electron beam, indicating that they are not the result of electron-induced faulting. The antigorite crystals of the sort shown in Figure 7 displayed modulation periodicities (*a* axes) of about 35–40Å. The image in Figure 7 was produced by tilting the crystal slightly out of orientation to enhance the contrast; a similar method was employed by Iijima and Buseck (1975) to improve the contrast of images showing enstatite stacking.

Although the periodicity of curvature reversal in the layers of classical antigorite is usually around 40Å, there are many areas in the serpentine of the Pelham specimen where the distance between reversals is much longer and non-periodic. In some places, this leads to kinks in the layer structure (Figs. 8a, 5d), and, in other places, regions without curvature reversal lead to orientation variations in the antigorite (Fig. 8b) or to a sinuous structure on a much larger scale than that of classical antigorite (Fig. 8b,c). More complete roll forms can also combine with the antigorite structure (Fig. 8d). All these observations shown in Figure 8 demonstrate that the antigorite structure can be intimately associated with serpentine having more extensive curving of the sheets, which is perhaps better thought of as local chrysotile structure. It is therefore necessary, at least in this case, to recognize a structural and hence stoichiometric continuum between the antigorite and chrysotile structures as classically defined by Whittaker and Zussman (1956).

Mechanisms of fiber formation in anthophyllite asbestos

It is clear from the microstructures in the Pelham anthophyllite that the primary mechanism for the formation of individual fibers must be the separation of the crystallites along grain boundaries. Most of these grain boundaries are structurally discontinuous, indicating that the bonding across the boundaries must be much weaker than in the bulk anthophyllite structure. Additionally, many of the grain boundaries between crystallites are filled with sheet silicates, possibly further reducing the cohesion between adjacent anthophyllite crystals. Furthermore, incipient disaggregation of the asbestos along the grain boundaries can be observed in the electron microscope as unfilled gaps between some crystallites; such gaps presumably were created during specimen preparation or handling. Separation along crystallite grain boundaries is also the most likely mechanism of fiber formation in the crocidolite examined by Alario Franco *et al.* (1977) and in the amosite of Zoltai (1979), which exhibited misorientation strongly

Fig. 5. Different grain-boundary types in anthophyllite asbestos. (a) Low-angle amphibole–amphibole grain boundary (about 0.5°) that is primarily coherent. The two crystals are separated by a series of partial dislocations, which are indicated by black arrows. The white line is parallel to the (010) traces, and the rotation between the crystals can be seen by sighting along this line at a low angle. (b) Amphibole–amphibole grain boundary with a higher angle (about 9°). The amphibole structure is primarily discontinuous across the boundary, except in the upper left, where two segments of the boundary are close to (010) of the two crystals. Triple- and quintuple-chain zippers terminate at the grain boundary. (c) An overview of grain boundaries between three crystallites (indicated by *a*- and *b*-axis orientations). The boundaries are partially filled by talc (T). Along most parts of the boundaries, the talc forms a planar coherent interface with one of the amphibole crystals. Terminations of chain-width defects (arrowed) can be seen in the largest crystal. (d) A grain boundary between anthophyllite (Anth) and antigorite (Atg). The layers of the antigorite structure are parallel to (210) of the anthophyllite. A large undulation is also present in the antigorite. (e) Grain boundary between two anthophyllite crystallites that is filled with talc. Extra layers (arrowed) with spacing of 5Å are probably brucite-like sheets, which locally produce a chlorite structural configuration.

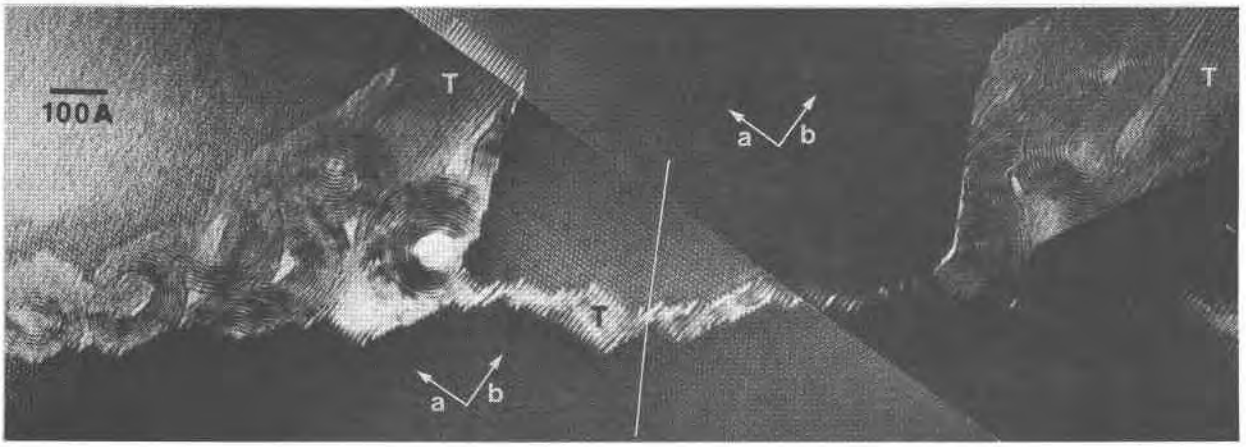

Fig. 6. Talc (T) and serpentine intergrown along a low-angle grain boundary between two anthophyllite crystals. The sharp line running diagonally across the figure is simply a photographic splice. The serpentine primarily has the curved forms of chrysotile. Incomplete chrysotile rolls can be seen in the large embayment of sheet silicate on the left side of the figure. In the embayment in the upper right, part of the serpentine possesses an S form, and two other rolls of chrysotile are intergrown to form a figure 8. The white line near the center of the figure follows the traces of (210) planes in the two anthophyllite crystallites; by viewing along this line at a low angle, the relative rotation between the two crystallites can be seen.

suggestive of the type of crystallite rotation microstructure evident in the Pelham anthophyllite asbestos. Indeed, it now seems likely that separation along grain boundaries of crystallites that are greatly elongated in the *c* direction is the primary mechanism for fiber formation in most, if not all, commercial-grade amphibole asbestos.

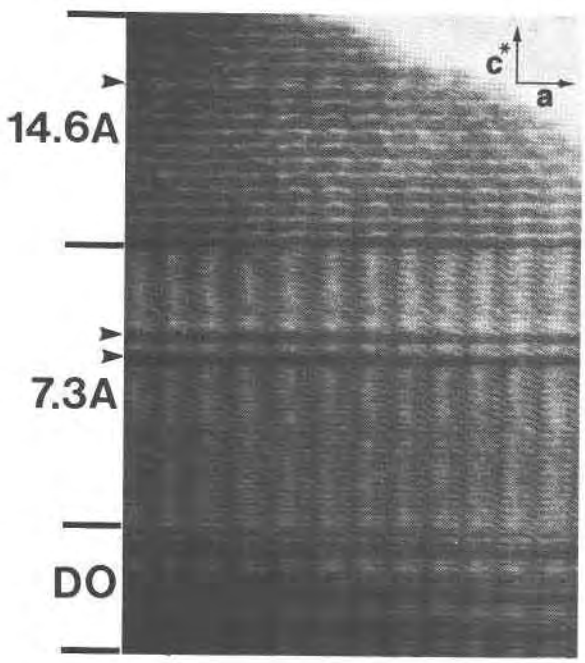

Fig. 7. Image of antigorite tilted slightly out of orientation to enhance contrast. Two ordered polytypes having basal spacings of 7.3 and 14.6Å are shown. Stacking faults in the ordered antigorite are indicated by arrows, and antigorite with disordered stacking is designated DO.

Yet not all fibrous anthophyllites possess the type of microstructure found in the Pelham specimen. Anthophyllite and associated wide-chain pyriboles from Chester, Vermont, do not contain rotationally disordered submicroscopic crystallites. It is true that this material is not a high-quality asbestos, but crystals with extensive chain-width disorder disaggregate with very mild crushing to fibers with high aspect ratios (as much as several thousand to one), many of which are extremely flexible. These physical properties underscore the observation of Zoltai (1979) that there may be a continuum of mechanical properties from asbestiform to brittle in amphiboles. Veblen *et al.* (1977) suggested several reasons why the mechanism of fiber formation in this specimen from Chester is breakage along the (010) chain-width errors and the (100) exsolution lamellae and stacking faults. First, partings parallel to (010) and (100) (Veblen and Burnham, 1978a) demonstrate that the Chester material does, in fact, break parallel to these planes, as well as breaking parallel to the ordinary (210) orthoamphibole cleavage planes. Such partings are not typical of most amphiboles, although tremolite polysynthetically-twinned on (100) and hornblende with (100) exsolution lamellae do commonly part on (100). In addition, it has been observed directly in the TEM where ledges occur on (100) and (010) crystal surfaces that the anthophyllite has, in fact, broken along stacking faults and chain-width errors (Fig. 9). One chain-silicate crystal may, in fact, split into nu-

merous smaller fibers, as shown in Figure 9b, which also suggests that the resulting fibers are flexible. Such breakage along defects presumably occurs because the stacking faults and wide-chain slabs in the anthophyllite structure represent planes of high energy, even though the crystal structure is completely continuous across these planes.

Note that not all anthophyllite that contains chain-width errors is as fibrous as the material from Chester. An anthophyllite from the Cascades, Washington (Veblen and Buseck, 1979b) contains a moderate number of such errors (fewer than the Chester amphibole) but tends to form acicular amphibole particles when crushed. This difference in mechanical behavior suggests that the energies of the chain-width errors are different in the two cases, leading to easier fracture in the Chester case, that the density of chain-width errors is an important parameter in the degree of fibrousness, or that some other factor, such as deformation history or minor chemical differences, may play a role in the physical properties of these amphiboles.

Although breakage along chain-width errors and twin planes or stacking faults may not be the primary mechanism of fiber formation in most commercial-grade amphibole asbestos specimens, such breakage may still occur and contribute to the fiber properties, even when most of the fiber separation occurs along grain boundaries. For example, further splitting of fibrils that have separated along grain boundaries may occur along chain-width errors and stacking faults during milling. Such defects appear to be nearly universal in commercial-grade amphibole asbestos, having been reported in many different specimens by competent electron microscopists (Chisholm, 1973, 1975; Hutchison *et al.,* 1975; Alario Franco *et al.,* 1977); in addition, of several other amphibole asbestos specimens I examined, all contain at least

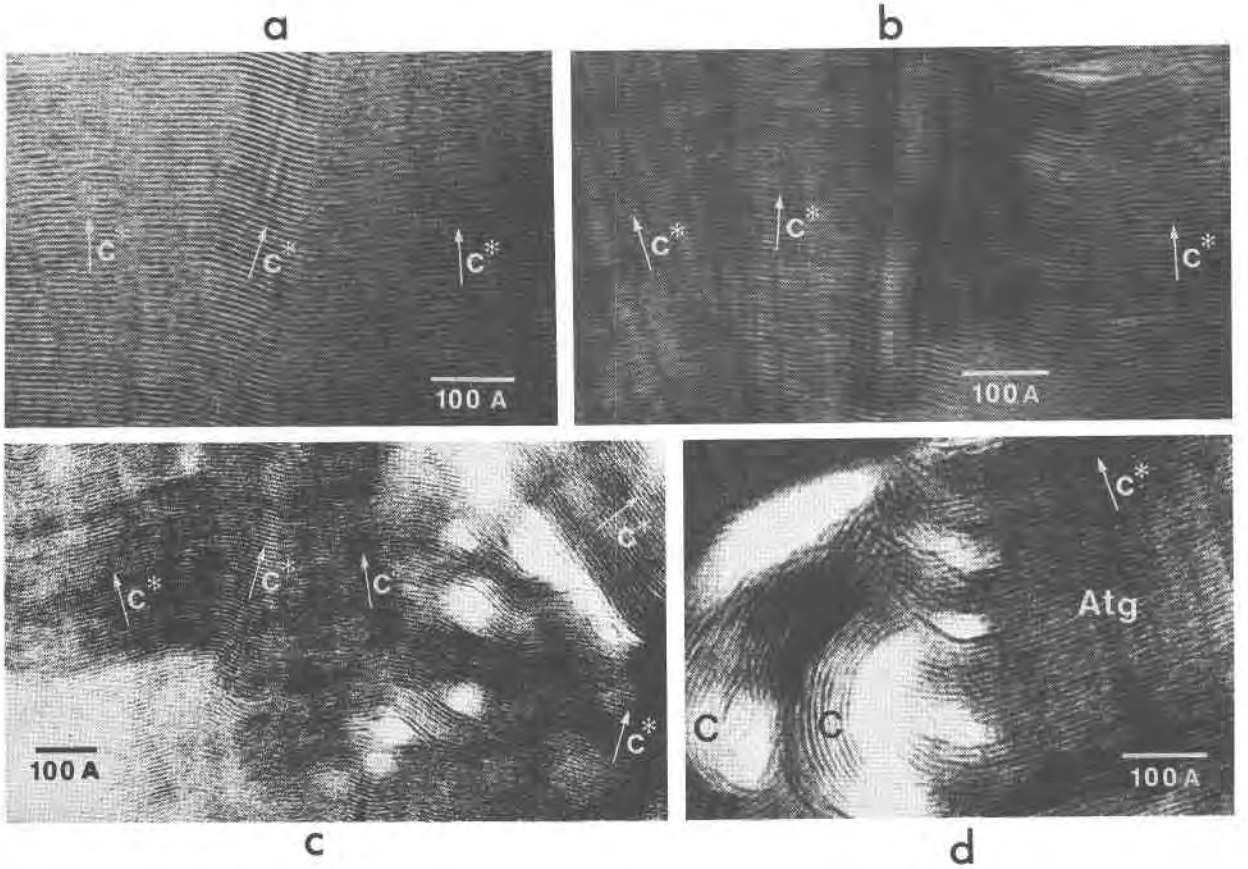

Fig. 8. Corrugation periodicity disorder and misorientation in antigorite. (a) A kink in the serpentine sheets. Local orientations of c^* are indicated. (b) Variation in layer curvature reversal can lead to orientation differences in different parts of an antigorite crystal. In the center and right portions of this figure the corrugation is nonperiodic, and the distance between curvature reversals is longer than that in typical antigorites. (c) Serpentine showing a highly sinuous arrangement of layers and resulting orientation differences. (d) Intergrowth of antigorite (Atg) and chrysotile (C) forms of serpentine.

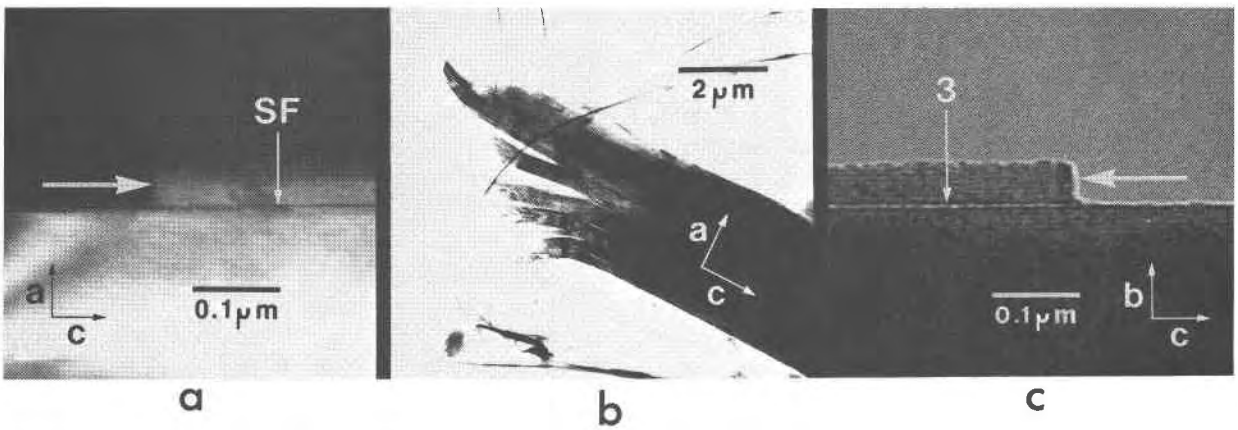

Fig. 9. Preferential splitting of anthophyllite from Chester, Vermont, along planar defects. (a) Multiple-beam dark-field image of a ledge on the edge of an anthophyllite crystal (shown by large white arrow) and its relationship to a (100) stacking fault (SF). The crystal has broken along the stacking fault. (The crystal appears light in this dark-field image.) (b) One end of an anthophyllite crystal splitting into several smaller fibers along planes parallel to (100). The bending associated with the splaying at the end of the crystal suggests that the thin fibers being formed will be flexible. (c) Single-beam bright-field image of an anthophyllite crystal that has partially split along a triple chain-width error (3). The large white arrow indicates a ledge on the edge of the crystal. (The crystal appears dark in this bright-field image.)

some chain-width errors and abundant (100) stacking faults or twin planes. These defects could thus provide important secondary mechanisms of fiber formation in high-quality amphibole asbestos.

The abundance of planar defects in amphibole asbestos contrasts sharply with the paucity or absence of such features in many massive amphiboles. It was, in fact, primarily this marked difference in planar defect abundance that led Veblen *et al.* (1977) to hypothesize that the primary mode of fiber formation in all amphibole asbestos is separation along planar defects. Even though fibers are probably commonly produced by separation along grain boundaries, the correlation between asbestiform habit and chain-width errors and stacking or twin faults must be explained. There are several possibilities for this correlation. One explanation is that the conditions of primary growth of amphibole asbestos of the Pelham type, with rotated fibrils, also favor the planar defects. The defects in asbestos with this type of microstructure would thus be formed during crystal growth, whereas the defects that produce fibrousness in amphiboles of the Chester type are formed subsequent to growth, during retrograde hydration reactions. Faulting during crystal growth may, in fact, be the best explanation for abundant (100) twin planes or stacking faults. It is probably easier, however, to explain at least some of the abundant chain-width errors in the Pelham anthophyllite as the products of retrograde reaction. Many of the microstructures associated with chain-width errors are similar to microstructures associated with pyribole alteration at other localities. Furthermore, alteration to talc, serpentine minerals, and chlorite has clearly taken place along most of the grain boundaries in the Pelham asbestos, and it is logical to assume that partial reaction by the introduction of chain-width errors took place at the same time. In fact, the extremely abundant, incoherent, high-angle grain boundaries in amphibole asbestos with this rotated-fiber microstructure provide excellent conduits through the asbestos for fluids that produce alteration. It is, in fact, hard to imagine alteration not taking place. Thus, it may be the permeability of much amphibole asbestos along high-angle grain boundaries that leads to the correlation between asbestiform habit and large concentrations of chain-width errors. On the other hand, some fibrous amphiboles, such as those from Chester, clearly acquire their errors in chain width without the benefit of such a cellular structure.

The role of surface defects

Preliminary tensile strength measurements of Walker and Zoltai (1979) have suggested that the ultimate strength of amphibole asbestos may exceed that of acicular amphibole crystals by as much as a factor of thirty. By analogy with strength enhancement in synthetically-prepared whiskers, it is argued that this difference results from a larger number of surface defects (Griffith cracks and dislocations impinging on the crystal surface) in the acicular amphiboles, as compared with their asbestiform counter-

parts. It is further suggested that the paucity of surface defects in amphibole asbestos is the primary cause of the asbestiform physical properties (Zoltai, 1979; Walker and Zoltai, 1979).

Such a systematic difference in surface defect densities may exist. There is, however, no direct TEM evidence to support such a conclusion. Such a strength difference may, instead, be a simple result of crystal size: with a dislocation density of $10^6/cm^2$, an asbestos fiber 0.1μm in diameter and 1cm long could be expected to have about 30 dislocations impinging on its surface; an acicular amphibole crystal 1mm in diameter of the same length and with the same dislocation density would have roughly 300,000 dislocations meeting its surface. If, in fact, tensile rupture tends to occur at dislocation-surface junctions, there are clearly many more possible sites for failure to be initiated in the acicular amphibole. The simple difference in surface/volume ratio might then account for the observed difference in strength. More detailed measurements of tensile strengths, coupled with TEM observations of dislocation and crystal surface ledge densities, should resolve this question.

It has not been experimentally demonstrated that there are systematic differences in dislocation densities between asbestiform and non-asbestiform amphiboles. It has, however, been shown conclusively that there are major microstructural differences. Specifically, there are extreme differences in the numbers of high-angle grain boundaries and/or planar defects. Almost certainly the individual amphibole fibers come apart along these weak boundaries more easily than massive amphibole can cleave, and these boundaries are therefore primarily responsible for the asbestiform physical properties. It is this ease of fiber separation that, even in hand specimen, obviously distinguishes amphibole asbestos from non-asbestiform varieties, not a secondary property such as tensile strength. Easy separation along planar defects may lead to crystal surfaces with fewer ledges than those formed by cleavage in acicular amphibole. Further investigations may therefore demonstrate such surface differences, but these differences could well be a consequence rather than a cause of the asbestiform habit.

Conclusions

Electron microscopy of an anthophyllite asbestos specimen from Pelham, Massachusetts, has revealed a wealth of complex microstructures. The specimen is composed primarily of submicron crystallites that are greatly elongated in the *c* direction and are rotated with respect to each other around axes close to *c*. The rotation between adjoining crystallites produces a variety of grain-boundary structures, and many of the grain boundaries contain intergrown sheet silicates. In places, these sheet silicates exhibit numerous complexities, including the intergrowth of antigorite and chrysotile structures.

The above microstructures strongly suggest that individual anthophyllite asbestos fibers form by separation along the weak, high-angle grain boundaries between crystallites. Investigations of anthophyllite from Chester, Vermont, on the other hand, have suggested that flexible fibers with very high aspect ratios can be produced by splitting along chain-width errors and (100) stacking faults (or twin planes in monoclinic amphibole). The problem of the mechanism of fiber formation in amphibole asbestos may, therefore, be a bit obstinate; instead of a single, simple explanation for the asbestiform habit, several separate mechanisms of fiber formation may operate either alone or in concert.

This paper has dealt primarily with anthophyllite. Complete characterization of microstructures in amphibole asbestos will require not only further observations on anthophyllite asbestos from other localities, but also investigations on other compositions, such as grunerite (amosite) and riebeckite (crocidolite). High-resolution electron microscopic observations on additional samples should enable a better evaluation of the factors controlling the asbestiform habit in amphiboles. Such work is currently in progress in this laboratory.

Acknowledgments

I thank amphibologists Peter Robinson, John Brady, and John Cheney for enthusiastically escorting me to the Pelham locality. I thank Peter Buseck for helpful collaboration on work with the Chester material, as described in Veblen *et al.* (1977). Microscopy was performed in the Arizona State University Facility for High Resolution Electron Microscopy, which was established with support from the NSF Regional Instrumentation Facilities Program, grant CHE79-16098. This work was supported by NSF grants EAR79-27094 and AENV76-17130, and by an Arizona State University Faculty Grant-in-Aid.

References

Alario Franco, M. A., J. L. Hutchison and J. M. Thomas (1977) Structural imperfection and morphology of crocidolite (blue asbestos). *Nature, 266,* 520–521.

Chisholm, J. E. (1973) Planar defects in fibrous amphiboles. *J. Mater. Sci., 8,* 475–483.

——— (1975) Crystallographic shear in silicate structures. In M. W. Roberts and J. M. Thomas, Eds., *Surface and Defect Properties of Solids, 4,* 126–151.

Hutchison, J. L., M. C. Irusteta and E. J. W. Whittaker (1975)

High resolution electron microscopy and diffraction studies of fibrous amphiboles. *Acta Crystallogr., A31,* 794–801.

Iijima, S. and P. R. Buseck (1975) High resolution electron microscopy of enstatite I: twinning, polymorphism, and polytypism. *Am. Mineral., 60,* 758–770.

Veblen, D. R. and C. W. Burnham (1978a) New biopyriboles from Chester, Vermont: I. Descriptive mineralogy. *Am. Mineral., 63,* 1000–1009.

——— and ——— (1978b) New biopyriboles from Chester, Vermont: II. The crystal chemistry of jimthompsonite, clinojimthompsonite, and chesterite, and the amphibole–mica reaction. *Am. Mineral., 63,* 1053–1073.

——— and P. R. Buseck (1979a) Chain-width order and disorder in biopyriboles. *Am. Mineral., 64,* 687–700.

——— and ——— (1979b) Serpentine minerals: intergrowths and new combination structures. *Science, 206,* 1398–1400.

——— and ——— (1979c) Replacement rules for hydration reactions in biopyriboles (abstr.). *Geol. Soc. Am. Abstracts with Programs, 11,* 532.

——— and ——— (1980) Microstructures and reaction mechanisms in biopyriboles. *Am. Mineral., 65,* 599–623.

———, ——— and C. W. Burnham (1977) Asbestiform chain silicates: new minerals and structural groups. *Science, 198,* 359–365.

Walker, J. S. and T. Zoltai (1979) A comparison of asbestos fibers with synthetic crystals known as "whiskers." *Ann. New York Acad. Sci., 330,* 687–704.

Whittaker, E. J. W. and J. Zussman (1956) The characterization of serpentine minerals by X-ray diffraction. *Mineral. Mag., 31,* 107–126.

Yada, K. (1979) Microstructures of chrysotile and antigorite by high resolution electron microscopy. *Can. Mineral., 17,* 679–691.

Zoltai, T. (1979) Asbestiform and acicular mineral fragments. *Ann. New York Acad. Sci., 330,* 621–642.

Manuscript received, March 17, 1980;
accepted for publication, June 9, 1980.